Egypt. J. Chem. **Vol. 66,** No. 3 pp. 465 - 478 (2023)

Egyptian Journal of Chemistry

http://ejchem.journals.ekb.eg/

Functionalization of Polyester Fabric with Green Synthesized Zinc Oxide Nanocomposites using Aloe-Vera Gel Extract Assisted by Microwave and Ultrasonic Techniques

Monira N. Michael[a], Eman M. Osman[a], Ibrahim El - T. El Sayed[b], Ahmed A. El Gokha[b], Seham A. Abu- Elanwar[a*]

[a]*Chemical Metrology Division, National Institute of Standards, Giza-12211, Egypt*

[b] *Department of Chemistry, Faculty of Science, Menoufia University, Shebin El Koom-13829, Egypt*

Abstract

Synthesis of inorganic/ organic nanocomposite using green route is a major focus of modern nanotechnology. Herein, we demonstrated the synthesis of ZnO NPs based on two different biopolymer matrices - hydroxyethyl methyl cellulose (HEMC) and chitosan (CS) - to produce two types of ZnO nanocomposites (ZnO/HEMC and ZnO/CS) utilizing Aloe-Vera plant extract as benign reducing agent of zinc acetate. The synthesis process and deposition of the synthesized ZnO nanocomposites into polyester fabric were performed in one pot to provide multifunctional polyester fabric. Moreover, microwave and ultrasonic irradiations are applied during the synthesis and finishing process as green physical techniques. ZnO nanocomposite treated samples were characterized via the following techniques: Scanning electron microscopy (SEM), X-ray diffraction (XRD), Fourier transform infrared spectroscopy (FTIR) and Atomic absorption spectroscopy (AAS). Transmission electron microscopy (TEM) images showed that ZnO nanoparticles in the prepared ZnO nanocomposites are mostly spherical and monodispersed with average particles size 4.1, 19.3, 28.5 and 54.2 nm. The performance of the treated samples was assessed through antibacterial activity, antistatic, UV protection and mechanical properties. The obtained results revealed successful functionalization of the polyester fabric and also, showed remarkable improvement in its performance which allows its usage in various fields such as medical textiles.

Keywords: ZnO nanoparticles; Hydroxyethylmethyl cellulose (HEMC); Chitosan (CS); Ultrasonic; Microwave; Polyester.

1. Introduction

Textile's functionalization with nanomaterials has been attracted lots of attention in recent years taking into consideration the environmental, quality and economic issues. Polyester fibers, the most widely used fibers in the textile industry in general, are used in the production of garments, curtains, clothes, automotive interiors and many other technical applications. ZnO nanostructure has gained substantial interest in the research community due to its biodegradability, low toxicity, economically effective and remarkable antimicrobial activity. So, it is widely used for various applications in textiles, cosmetics, pharmaceutical, electronics, sensors and food industries [1-4]. ZnO is known to be one of the most important semiconductor with a band gap of (3.3 eV), an excitation binding energy of (60 meV) at room temperature, and also has excellent thermal and chemical stability [5, 6]. Green synthesis of metallic nanoparticles using plants has become an interesting aspect as the process has significant potential and a number of advantages relative to the conventional chemical and physical methods that are often costly and potentially harmful to the environment [7]. Plants possess various biomolecules and metabolites like proteins, vitamins, flavonoids and polysaccharides [8 -10]. These plants metabolites contain polar functional groups, such as carboxyl, hydroxyl and amino groups that are capable of interacting with metal ions through different mechanisms such as reduction, complex/chelate formation, ion exchange, sorption, electrostatic attraction, covalent bonding, Van der Waals attraction and precipitation [11]. Also, these molecules play a pivotal role in the capping of the produced nanoparticles which is important for stability and biocompatibility [12, 13]. Aloe Vera is a hardy, perennial, tropical, drought-resistant, succulent plant. It has anti-inflammatory, antiviral and antibacterial properties. Several studies have revealed that Aloe Vera gel contains numerous potentially active ingredients such as vitamins, amino acids, phenolic compounds, lignin, saponins, sterols, flavonoids,

*Corresponding author e-mail:sahmedradi71@gmail.com.
Receive Date: 16 June 2022, Revise Date: 19 July 2022, Accept Date: 21 July 2022
DOI: 10.21608/EJCHEM.2022.145123.6329

enzymes and organic acids, which have an essential role in the green synthesis of nanoparticles and stabilizing it [14-17].

Biodegradable polymers like Chitosan (CS) and Hydroxylethylmethyl cellulose (HEMC), have much attention in recent years in the synthesis of nanoparticles because of their excellent biocompatibility and low toxicity even after degradation. They are considered green, natural and inexpensive polysaccharides. Chitosan is the 2nd most available natural polymer after cellulose and is obtained by alkaline *N* -deacetylation of chitin. It is structurally analogous to cellulose with acetamido or amino groups instead of hydroxyl groups at C-2. Chitosan (CS) and Hydroxylethylmethyl cellulose (HEMC) were used in the current study as matrices for nanoparticles incorporation. Several research groups have revealed that they can act as mild reducing and stabilizing agents for the green synthesis of nanoparticles [18-20]. Microwave and ultrasonication are considered simple green physical tools for enhancing nanoparticles synthesis. The basic mechanisms of microwave-assisted synthesis are polarization and conduction. The materials with large dipole moments, such as water, are rotated or vibrated vigorously in the presence of a magnetic field caused by the frequency of the alternating current of a microwave and are then heated by quick energy conversion from the above kinetic energy. So, the microwave ensures more uniform and rapid heating than conventional heating [21-24]. Ultrasonication is performed to achieve multiple purposes including deagglomeration, dispersion and size reduction of the formed nanoparticles. Also. It is considered an effective technique for the deposition of nanomaterials on the surface of various substrates [25]. Ultrasonication generates acoustic cavitation in the solution and in turn, leads to formation of microjets and shock waves with high pressure and high velocity. These microjets are capable of projecting the nanoparticles toward the surface of a substrate at a speed sufficient to adhere them strongly. The bonding involved can be either physical or chemical depending on the nature of the substrate [26, 27].

In this research work, polyester fabric was functionalized with two ZnO nanocomposites (ZnO/ CS and ZnO/ HEMC) which were synthesized through a green approach using the gel aqueous extract of Aloe-Vera plant as benign reducing and capping agent. Synthesis and functionalization were carried out in the same pot with the aid of microwave and ultrasonication for reducing the reaction time and energy, as well as eliminate the use of hazardous chemicals such as carriers.

2. Experimental

2.1. Materials and chemicals

Bleached and scoured 100% polyester knitted fabric (weight 167 g/m^2, thickness 0.446 mm) was purchased from Abou El-Ola for Spinning and Weaving, 10th of Ramadan, Egypt. Zinc acetate dihydrate (CDH Ltd. India) was used as ZnO precursor. Medium molecular weight chitosan - with a degree of N-acetylation of DA= 85% - and hydroxyethyl methyl cellulose (PVT Ltd. India) were used separately as polymer matrices. Acetic acid and sodium hydroxide were of analytical grade and used as purchased without further purification. Fresh and healthy Aloe-Vera leaves were collected from the local farming community.

2.2. Methods

2.2.1. Preparation and specification of the reaction mixtures

a) Aloe Vera gel leaves extract preparation

The collected Aloe Vera leaves were washed very well with running tap water followed by distilled water. The gel was collected from the leaves by peeling off the outer green skin layer and chopped in a blender. Then, mixed with distilled water using a ratio of 2:1 and the mixture was boiled for 20 minutes with continuous stirring. Finally, the mixture was filtered using nylon mesh followed by centrifuging at 4000 rpm for 30 minutes and the clear extract was stored at 4 ^{o}C till further use.

b) HEMC solution preparation

HEMC stock solution (0.5%) was prepared by dissolving 1.0 gram HEMC powder in 200 ml distilled water using a magnetic stirrer at 40 ^{o}C till completely dissolved.

c) Chitosan solution preparation

Chitosan stock solution (0.25%) was prepared by dissolving 0.5 gram chitosan powder in 200 ml distilled water containing 2ml acetic acid using a magnetic stirrer at 40 ^{o}C till completely dissolved

d) Reaction mixtures preparation

Four reaction mixtures were prepared as illustrated in Table 1 at room temperature using a magnetic stirrer for homogenizing and NaOH for adjusting pH.

2.2.2. Nanocomposites synthesis and fabric samples functionalization

Four polyester fabric samples S1, S2, S3 and S4 were immersed into four reaction mixtures RX1, RX2, RX3 and RX4, respectively as clarified in Table 1 using material to liquor ratio 1:50. The four reaction mixtures containing the fabric samples were placed into the microwave oven at a power 800 Watt for 4 minutes to assist the nanoparticles formation. The temperature of the reaction mixtures reached ≈ 85^{o}C and their colour changed, left to cool at room temperature, then, subjected to sonication (ultrasonic processor 500 Watt model, operating at 20 kHz,

standard probe 13mm in diameter) for 15 minutes at 70% wave amplitude in an ice bath to maintain the solution at low temperature (< 20 °C). Finally, the treated fabric samples are washed thoroughly with distilled water to remove the by-products and the loosely bound materials. Then, dried at room temperature for characterization.

Table 1. Codes for the treated fabric samples and their residual reaction mixtures.

RX	The reaction mixture (RX) Identity	pH	Residual reaction mixtures codes	The treated polyester samples codes
1	2 grams ZnA/55ml D.W. + 15 ml AV extract + 30 ml HEMC solution	6.6	RX1	S1
2	2 grams ZnA/55ml D.W. + 15 ml AV extract + 30 ml HEMC solution	8	RX2	S2
3	2 grams ZnA/55 ml D.W. + 15 ml AV extract + 30 ml CS solution	6.6	RX3	S3
4	2 grams ZnA/55 ml D.W. + 15 ml AV extract + 30 ml CS solution	8	RX4	S4

Where RX=Reaction mixture, ZnA =Zinc acetate, D.W. = Distilled water, AV= Aloe Vera extract.

2.3. Testing and Analysis

2.3.1. Evaluation of the residual reaction mixtures

2.3.1.1. UV-Visible spectrum

The optical absorbance of the synthesized nanocomposites in the residual reaction mixtures was performed using UV-visible spectrophotometer (Thermo Scientific - Helios gamma - IRV) with a wavelength range of 280 - 400 nm at Cairo University Research Park (CURP).

2.3.1.2. Transmission electron microscopy (TEM)

The surface morphology and size of the synthesized nanocomposites in the residual reaction mixtures were analyzed by transmission electron microscopy (JEM-1400, JEOL Ltd., Japan) with an accelerating voltage of 80 kV at CURP. The specimens of TEM measurements were prepared by depositing a drop from the examined residual reaction mixture on Cu grid coated by an amorphous carbon film in order to provide good conductivity for electron beam and dried in air at room temperature.

2.3.2. Evaluation of the treated fabric samples

2.3.2.1. Scanning electron microscope (SEM)

The surface morphology of the selected treated fabric samples was observed on SEM (JSM-5200 Scanning Microscope, JEOL Ltd., Japan) at CURP, using magnification x1500, scan width 10 µm and accelerating voltage 20-25 kV. All the samples were coated with gold film under vacuum before SEM testing.

2.3.2.2. X-ray diffraction (XRD) analysis

The X-ray powder diffraction patterns of the untreated and treated fabric samples were measured using a (Scintag Inc., USA) diffractometer at Reference Lab., National Institute of Standard (NIS). The 2θ scan was performed in the angular range of 10˚–80˚ with a scanning rate of 2˚/min, using CuKα as a radiation source of wavelength (λ = 1.5418 Å). The degree of crystallinity (X_c) of the samples under investigation was calculated from the XRD intensity data using Segal's formula [28]:

$$X_c = [I_c / (I_c + I_a)] \times 100 \quad \text{Equation (1)}$$

Where I_c and I_a are the integrated intensities of crystalline and amorphous parts of the samples, respectively.

2.3.2.3. Fourier transform infrared spectroscopy (FTIR)

FTIR spectra of untreated and treated polyester samples were recorded in the transmittance mode with attenuated total reflectance (ATR) using zinc selenide crystal. The spectra were taken in the wavelength range of 400–4000 cm^{-1} at room temperature using the KBr pellet technique. The measurements were carried out using Nicollet 380 FTIR spectrophotometer at Material Testing Lab., National Institute of Standards (NIS).

2.3.2.4. Atomic absorption spectroscopy (AAS)

AAS is an analytical technique used for the quantitative determination of a particular element in a sample. It is based on the absorption of light by free metallic ions. Thus, the zinc content of the treated fabric samples was determined using a flame atomic absorption spectrometer (ZEEnit 700 P, Analytik Jena, Germany) at Reference Lab., NIS.

2.3.3. Performance properties evaluation of the treated fabric samples

2.3.3.1. UV protection property

It is one of the most important qualifications, especially for the textiles used under the conditions of prolonged sun exposure and is defined in terms of ultraviolet protection factor (UPF). It was measured

for all samples under investigation using UV Shimadzu spectrophotometer according to the standard test method of (AATCC 183-2004) at photometry Lab., NIS.

2.3.3.2. Antibacterial activity

Antibacterial activity was evaluated qualitatively for the treated fabric samples towards two strains of Gram-positive (Staphylococcus aureus) and Gram-negative (Escherichia coli) using disc diffusion method on nutrient agar [29-31], according to AATCC Test Method 147-2004. Antibacterial activity was measured as the diameter of the inhibition zone in three different fixed directions and the mean diameter was recorded and expressed in millimeters, taking into account that the sample diameter was 15 mm. The durability of antibacterial finishing of treated fabric samples was assessed after 5 and 10 washing cycles using AATCC 61(2A) standard test method.

2.3.3.3. Air permeability

Air permeability is described as the rate of air flow passing perpendicularly through a known area of the fabric when there is different air pressure on either surface of the fabric and affected by the fabric porosity [32, 33]. Air permeability of the examined fabric samples was measured using SDL Air Permeability Tester, England, according to ASTM D737- 04 (2008) standard Method at Material Testing Lab., NIS.

2.3.3.4. Water absorption

The water absorbency of the examined fabric samples is investigated according to the AATCC test method 79-2007. This test method is designed to measure the time required for water droplet falls from a distance of 1cm on a taut fabric surface to be completely absorbed into the fabric. Five measurements were averaged and recorded as wetting time [34].

2.3.3.5. Antistatic property

The static electricity level of the examined samples can be digitally reflected by measuring electrostatic potentials using Electrostatic Fieldmeter (FMX-003, SIMCO, Japan) at Material Testing Lab., NIS.

2.3.3.6. Mechanical Properties

The bursting strength of the examined knitted fabric samples was evaluated according to ISO 13934-2:1999 standard method using a universal testing machine (Tinius Olsen, H5KT, UK) at Material Testing Lab., NIS.

3. Results and Discussion

3.1. Characterization and evaluation of the residual reaction mixtures

3.1.1. UV–Vis spectroscopy

Visual colour change of the reaction solutions is the initial indication of nanoparticle synthesis [35]. The colour of the reaction mixtures changes during the synthesis of ZnO nanocomposites from faint yellow to yellowish white at pH6.6 and to milky white at pH8 as demonstrated in Figure 1(a), indicating more ZnO nanoparticles are formed at pH8 which may be due to the reactivity of the reductant increased in alkaline medium. It is believed that the green synthesis process of ZnO from ZnA is divided into three steps which are hydrolysis, complexation and decomposition. The first step is the hydrolysis of zinc acetate to its ions, followed by the reaction between the hydroxyl groups of phenolic compounds from the plant extract with Zn2+ to form Zn complex through chelation. Zn complex received π electrons donated by carbonyl groups from biomolecules, resulting in the reduction of Zn^{2+} ions to Zn^{0} and finally, decomposition of Zn complex to ZnO Nps under the effect of microwave irradiation and this is confirmed by the colour change of the reaction mixture [36].

The maximum absorbance peaks of the residual reaction mixtures RX1, RX2, RX3 and RX4 in the UV–Vis spectrum are observed at 306, 296, 336 and 312 nm, respectively, as clarified in Figure 1(b & c). This indicates that, the green synthesis of ZnO Nps occurred at a lower wavelength compared with that synthesized by chemical routes (340–390 nm) [37]. This may be due to the capping of the synthesized ZnO NPs with the biomolecules of the plant extract and/or the interaction with the biopolymer as reported in some published literature [1, 3, 4]. Also, the absorption peaks of residual reaction mixtures at pH8 appeared at a lower wavelength and higher intensity than that at pH6.6 because a higher pH (alkaline) facilitates the nucleation and consequently the formation of a large quantity of smaller and highly dispersed nanoparticles. While, at lower pH (acidic) nanoparticle aggregation is preferred over nucleation i.e. larger-sized nanoparticles are observed at lower pH [38]. Further, the single and narrow peaks appeared, proving the spherical shape and narrow size distribution of the synthesized nanoparticles [39, 40].

3.1.2.TEM analysis

TEM images of the residual reaction mixtures RX1, RX2, RX3 and RX4 are presented in Figure 2. It is clearly observed that the ZnO nanoparticles in the prepared ZnO nanocomposites are mostly spherical

and monodispersed with average sizes of 28.5, 4.1, 54.2 and 19.3 nm, respectively. Also, it is found that the particle size of the formed nanoparticles at pH8 is smaller than their corresponding at pH6.6 i.e. RX2 < RX1 and RX4 < RX3. These results have supported the results obtained from the UV-Vis study.

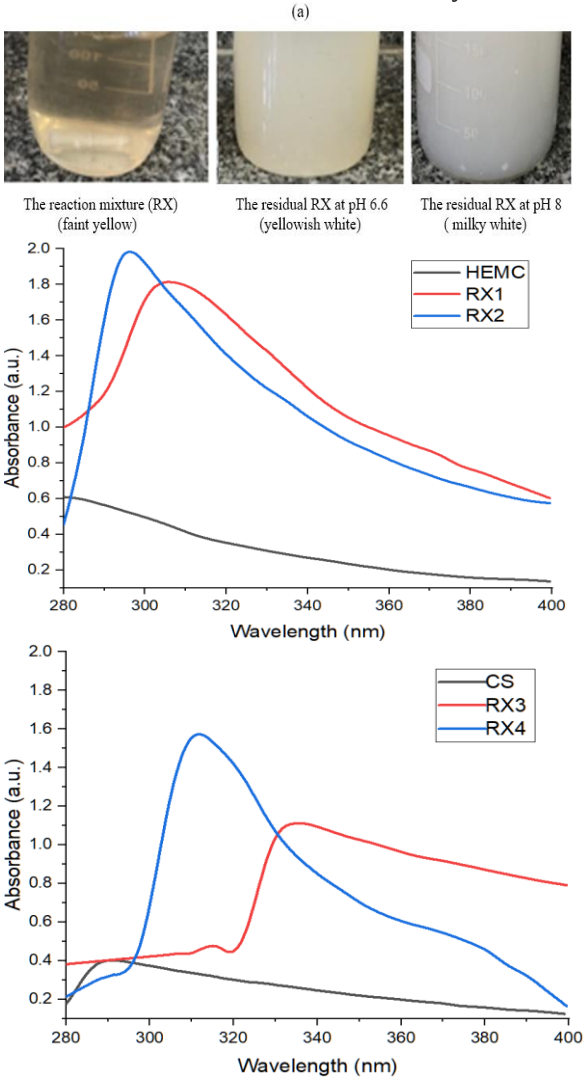

Figure 1. (a) Colour changes of the residual reaction mixtures, UV-Vis absorption spectra of (b) HEMC, RX1 & RX2, (c) CS, RX3 & RX4

(RX1)

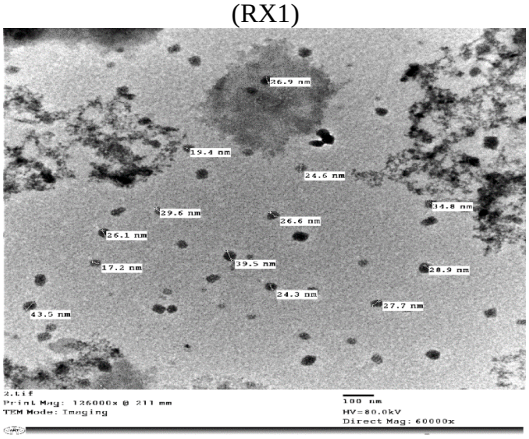

(RX2)

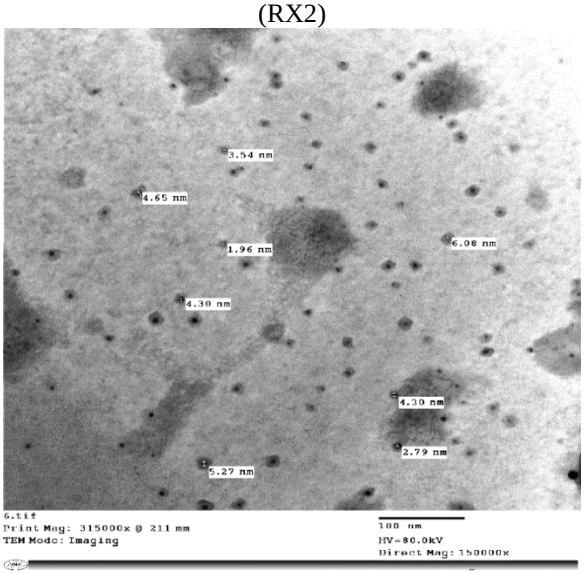

(RX3)

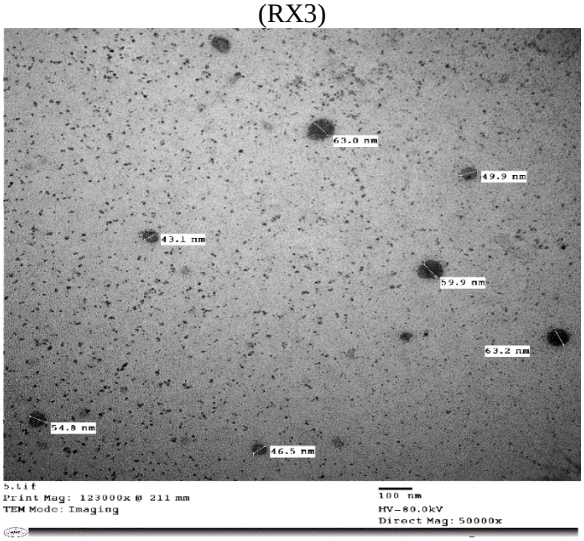

(RX4)

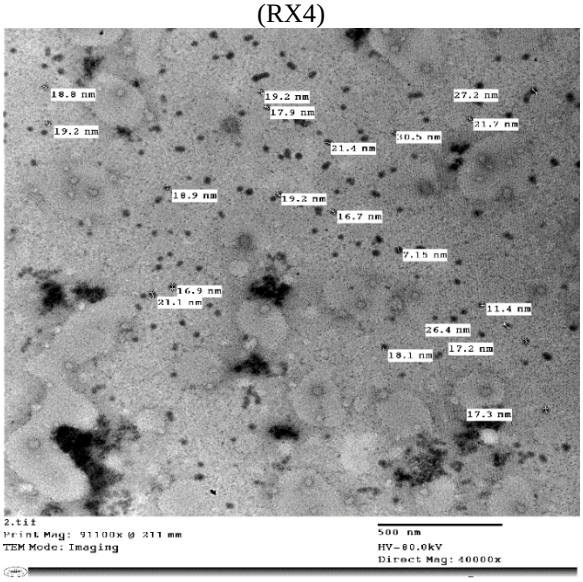

Figure 2. TEM images of the residual reaction mixtures RX1, RX2, RX3 and RX4

3.2. Characterization and evaluation of the treated fabric samples

3.2.1. SEM analysis

The morphology of untreated and the treated polyester fabric samples (S1, S2, S3 & S4) are inspected by SEM with magnification power x1500, and the obtained images are shown in Figure 3. The visual observation of the SEM images expressed that the untreated polyester sample has a long fibril structure arranged in order with a clear and smooth surface. While, the treated samples showed that the synthesized ZnO nanocomposites are incorporated in its fibers and dispersed on its surface with low agglomerations. Besides, its fibril structure is swelled to some extent in comparing with the untreated ones. Also, the treated samples S2 and S4 showed more deposition of ZnO nanocomposites than S1 and S3, this is attributed to smaller particles size with higher surface area are formed at pH8. This result is in agreement with that obtained from UV-Vis analysis.

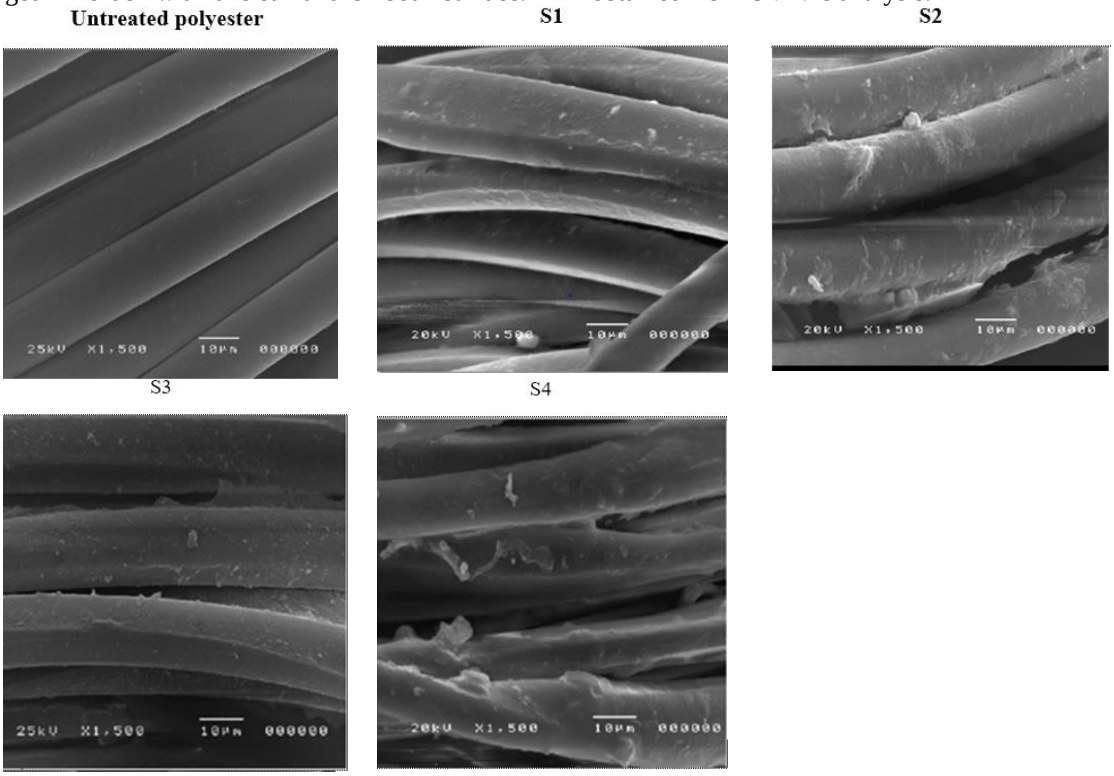

Figure 3. SEM images of untreated and ZnO nanocomposite treated polyester samples (S1, S2, S3 & S4).

3.2.2. XRD analysis

XRD analysis is used to prove the crystalline structure of the biosynthesized ZnO Nps in ZnO nanocomposite and investigate the crystallinity changes in the treated polyester samples**.** As shown in Figure 4, XRD patterns of both native HEMC and native chitosan exhibited one characteristic broad diffraction peak at $2\theta \approx 20^{o}$ [41]. It is clear that, all diffraction patterns of the examined fabric samples exhibited three intense peaks at 2θ position 16^{o}, 22^{o} and 25^{o} corresponding to the crystalline structure of polyester fabric [42]. Additional peaks appeared at 2θ positions of 31.5^{o}, 34.2^{o}, 36^{o}, 56.4^{o}, and 62.6^{o} corresponding to lattice planes (100), (002), (101), (110) and (103), respectively for S1 sample and 2θ position of 31.5^{o}, 34.1^{o}, 36.04^{o}, 47.8^{o}, 56.4^{o}, 62.7^{o} and 67.8^{o} corresponding to lattice planes (100), (002), (101), (102), (110), (103) and (112), respectively for S2 sample. While S3 sample exhibited peaks at $2\theta = 32.7^{o}$ and 55.3^{o} corresponding to lattice planes (100) and (110), respectively. S4 sample showed peaks at 31.7°, 34.2°, 36.2°, 48°, 56.4°, 62.6° and 67.8° corresponding to lattice planes (100), (002), (101), (102), (110), (103) and (112), respectively.

All the diffraction peaks of S1, S2, S3 and S4 are in good agreement with those of hexagonal wurtzite structure of ZnO NPs according to the Joint Committee on Powder Diffraction Standard (JCPDS) No. 36-1451 [43,44]. Also, it is noted that the number of peaks in case of the treated samples S1 and S3 is less than the number of peaks in S2 and S4 samples, revealed incomplete reduction of ZnA to ZnO NPs at pH 6.6. Moreover, some impurity peaks can be seen due to the plant extract residues

Table 2 summarizes the peak intensities and crystallinities of all the examined samples. It can be clearly observed that the intensity of the characteristic peaks of polyester at $2\theta = 22^{o}$ and 25^{o} are decreased after treatment, while the intensity of the peak at

$2\theta=16^{o}$ is increased and the diffraction peak of either HEMC or CS was not found. This can be attributed to the interaction between the synthesized ZnO nanoparticles with the biopolymers (HEMC and CS) to produce ZnO/HEMC and ZnO/CS nanocomposites. This led to shifting the peak that belongs to HEMC and CS from $2\theta \approx 20^{o}$ to $2\theta = 16^{o}$, causing a remarkable increase in its intensity as shown in Figure 4 and Table 2. Moreover, the shape of this peak ($2\theta = 16^{o}$) became pointed and narrow, indicating that the crystallinity of the treated polyester samples increased. The degree of crystallinity (X_c) of all examined samples is calculated using equation (1), and follows the following ranking order:

$(X_c)_{S2} > (X_c)_{S1} > (X_c)_{Untreated}$ and $(X_c)_{S4} > (X_c)_{S3} > (X_c)_{Untreated}$. This means that more ZnO nanocomposites are deposited into fabric samples at pH8 than their corresponding at pH6.6, leading to increase in the surface area per unit volume, accordingly higher degree of crystallinity is obtained. All the aforementioned results confirmed that the synthesized ZnO nanocomposites are successfully incorporated into polyester fabric samples without any change in the structural regularity of the main chains of polyester.

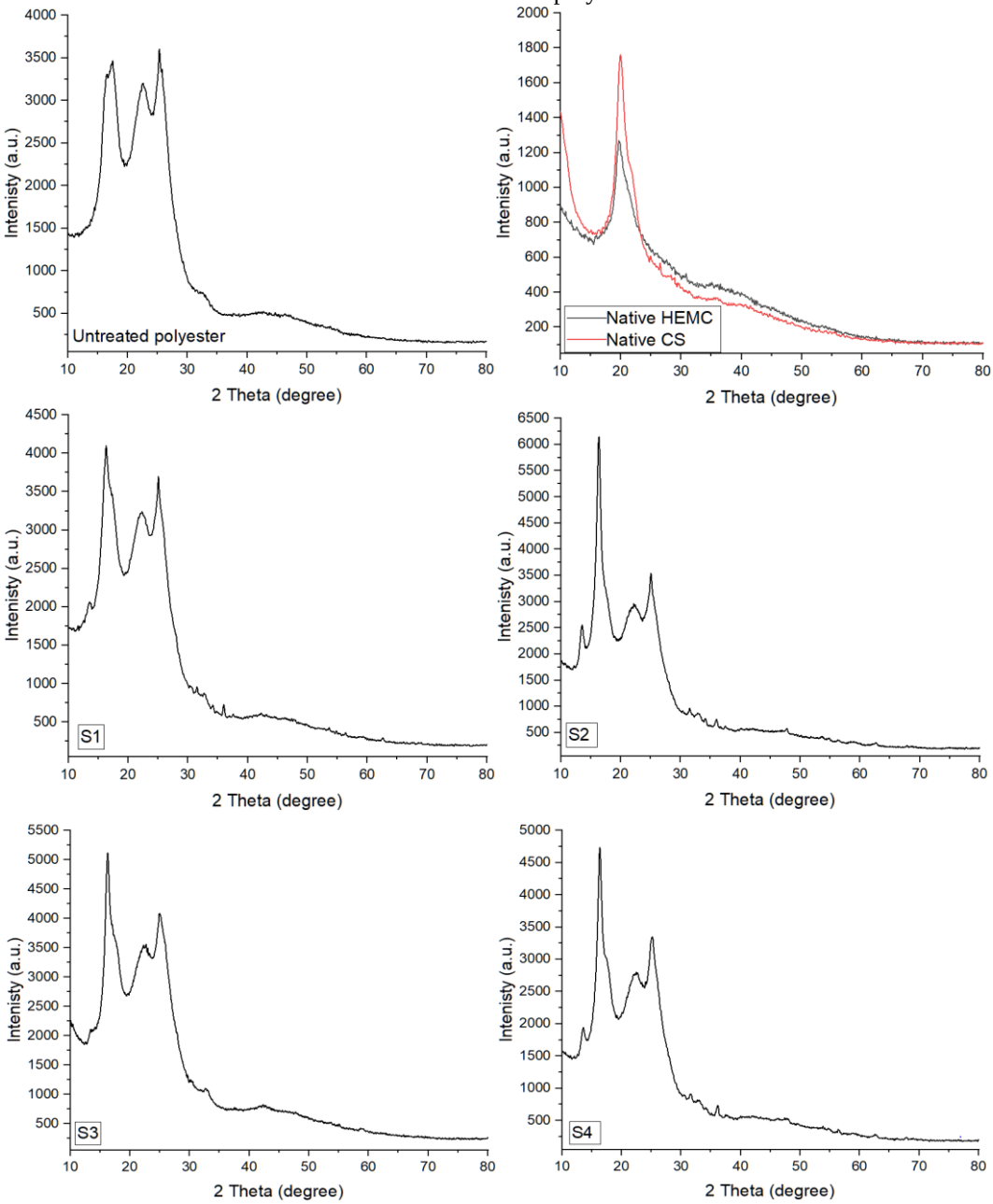

Figure 4. XRD patterns of Native HEMC and chitosan, untreated and ZnO nanocomposite treated fabric samples (S1, S2, S3 & S4)

Table 2. Peak intensities and crystallinities of the examined polyester fabric samples

Sample´s code	Peak´s intensity values at 2θ position ≈				The degree of crystallinity (%)
	16°	20°	22°	25°	
Untreated	74.98	-	66.72	100	59.98
S1	100	-	58.81	96.42	62.97
S2	100	-	22.75	46.01	81.47
S3	100	-	41.98	69.52	70.43
S4	100	-	34.45	61.04	74.38
HEMC	-	100	-	-	-
CS	-	100	-	-	-

3.2.3. FTIR - ATR analysis

FTIR is performed to identify materials composition and functional groups present in a sample, it is a fingerprint of all types of organic compounds and some inorganic compounds [45]. Both the untreated and treated polyester samples are characterized by FTIR spectroscopy to confirm the chemical interaction between the synthesized ZnO nanocomposites and the fabric. Figure 5 shows the FTIR spectra of untreated and all ZnO nanocomposite treated fabric samples (S1, S2, S3 and S4). There are common peaks between polyester, HEMC, CS and phytochemicals in Aloe Vera gel extract which are O-H, C-O, C-C-O and C-H. In addition to N-H and C=O groups which attributed to acetamido group in CS and amino acids in AV extract.

All samples showed Three strong bands at 1712, 1243 and 1090 cm^{-1} attributed to the asymmetrical stretching vibration of C=O, C–O and C–C–O respectively, which are characteristic for both ester linkage and carboxylic acid groups. While, the peak located at ≈1012 cm^{-1} is attributed to O-H out of plane bending in terminal carboxylic. There was a broad band in all treated samples around 3432 cm^{-1} corresponding to the combined peaks of O–H and N–H stretching vibration groups. Whereas, the small peak at 1577 cm^{-1} is related to the coupling interaction between the two equivalent carbon bonds of carboxylate anion. Another two small peaks at ≈ 2966 and 2910 cm^{-1} are attributed to aliphatic CH_2 and CH_3 stretching vibration, respectively. Also, C–H bonds of the benzene rings are observed around 1410-1510 cm^{-1}. While, C-H bending and out of plane C-H bending vibrations appeared at ≈725 cm^{-1} and near 600-420 cm^{-1}, respectively. In addition, Out of plane C-C bending vibration and C=C bond appeared at 873 and 967 cm^{-1}, respectively [46.47].

FTIR spectra of all treated samples are similar to the untreated ones, except for the changes in the intensity and broadness of some bands, indicating that the interaction between the synthesized ZnO nanocomposites and the functional groups of polyester occurred without structural change in the polyester chain. The intensities of the common peaks are listed in Table 3 and the obtained data demonstrated that the treated samples had higher peak intensity values than the untreated ones, due to the additional functional groups from plant extract and biopolymers. Also, the intensity values of the peaks in S2 and S4 samples are higher than that in S1 and S3 samples, indicating that more ZnO nanocomposites have adhered to fabric samples at pH 8. Moreover, the change in the shape of some peaks especially at wavenumber ≈ 500 cm^{-1}, indicates the presence of (Zn–O) stretching of ZnO nanoparticles, where, metal oxides stretching vibration bands are found at low wavenumber around 400–800 cm^{-1} range according to the previous literature [48]. While, the change in the broadening of the band at wavenumber 3432 cm^{-1} proved the capping of ZnO Nps with of O-H and N-H groups. All the aforementioned results confirmed that the synthesized ZnO nanocomposites are successfully incorporated into polyester fabric samples by electrostatic interactions between the components without any change in structural regularity of the main chains of polyester, this is in agreement with the results obtained from XRD analysis.

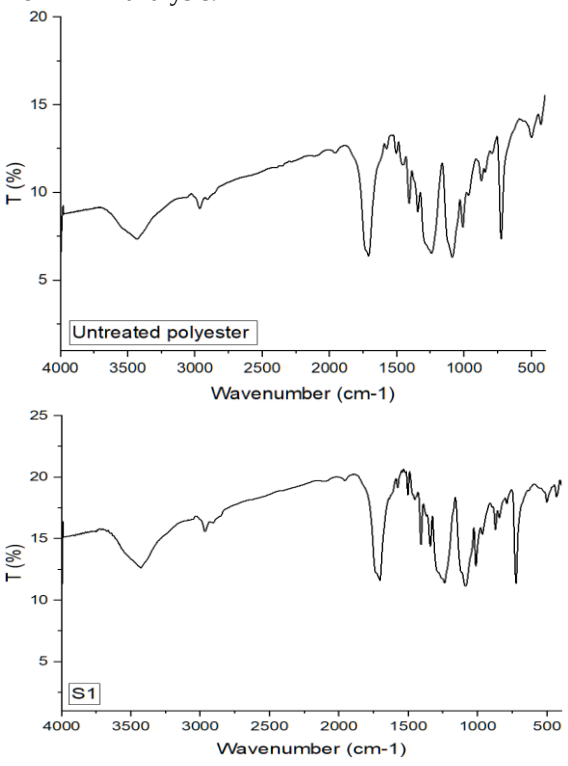

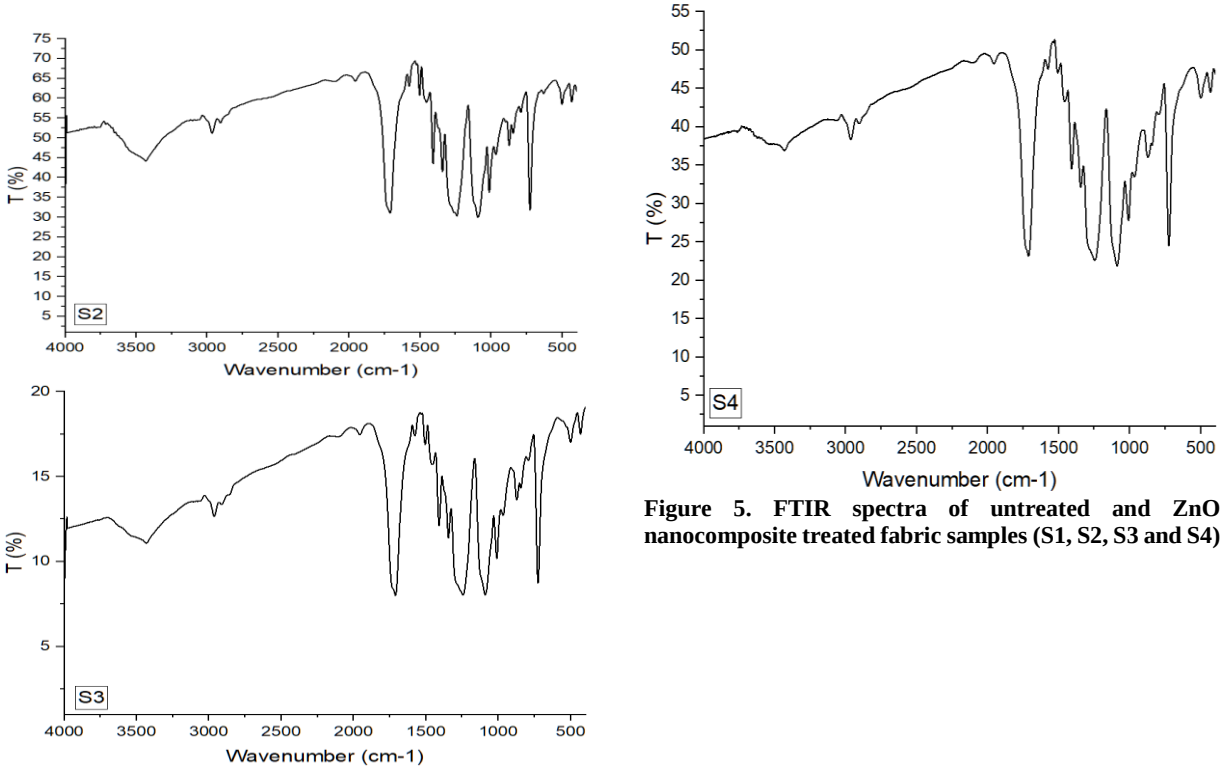

Figure 5. FTIR spectra of untreated and ZnO nanocomposite treated fabric samples (S1, S2, S3 and S4)

Table 3. FTIR characteristic peaks of the examined polyester samples and their intensity values.

Characteristic chemical group	Wavenumber (cm^{-1}) ≈	The peak's intensity				
		Untreated	S1	S2	S3	S4
O - H & N – H Stretching vibration	3432	7.36	12.64	44.25	11.08	36.92
C-H Stretching vibration(CH2&CH3)	2966 & 2910	9.10 & 9.63	15.59 & 16.27	51.28 & 53.93	12.70 & 13.36	38.31 & 40.42
C=O stretching vibration	1712	6.39	11.59	31.00	8.00	23.17
C-H of benzene ring	1410	9.39	14.31	46.32	12.11	34.50
C-O stretching vibration	1243	6.55	11.62	30.50	8.03	22.60
C-C-O stretching vibration	1090	6.32	11.15	30.02	8.04	21.89
O-H out of plane bending	1012	8.06	12.65	38.05	10.19	27.97
C=C stretching vibration	967	9.86	15.34	46.27	12.72	33.52
C-C out of plane bending	873	10.69	15.45	49.61	13.63	36.03
C-H bending	725	7.38	11.24	33.95	8.74	24.52
C-H out of plane bending	500 & 430	13.15 & 13.38	17.87 & 18.27	59.13 59.79	17.02 & 17.49	43.79 & 44.54

3.2.4. AAS analysis:

It is used for the quantitative determination of Zn element in the polyester fabric after treatment. The results indicated that the Zn content per 0.2 gram fabric sample in percentage was 0.4782, 0.6881, 0.3815 and 0.6103 for S1, S2, S3 and S4, respectively. Also, it is easily noticeable that Zn content of S2 and S4 samples was higher than S1 and S3 samples, respectively, indicating more ZnO nanocomposites are formed at pH8. This result was well consistent with the above mentioned experimental results.

3.3. Performance properties evaluation

3.3.1. UV-protection

The capability of fabric to block UV radiation depends on several parameters such as nature of fibers, fabric construction, thickness, colour depth and finishing agents [49-52]. Table 4 shows the sun protection values of the clothing according to AS/NZS 4399:1996 standard [41].

Table 4. Classification of clothing according to UPF values

UPF values	UPF rating
15-24	Good protection
25-39	Very good protection
40-50+	Excellent protection

UPF values as UVA and UVB blocking percentages of untreated and treated polyester samples are demonstrated in Table 5. The obtained data shows that the untreated fabric sample has poor protection against UV radiation, this is attributed to the nature of the knitted fabric structure, i.e. high porosity and elasticity with low dimensional stability [53]. While, the UPF values of treated samples are better than the untreated ones due to the inherent scattering and high UV absorbance properties of ZnO nanocomposites [41, 54]. Also, it is found that S2 and S4 samples have higher UPF values than S1 and S3, respectively, these results are compatible with AAS results i.e. the higher Zn content the better UPF values [55].

Table 5. UPF values of untreated and treated fabric samples.

Sample Code	Average UVA	Average UVB	Average UPF	Rating
Untreated	17.67	6.16	13.24	poor
S1	9.44	4.31	19.92	Good
S2	6.18	2.45	34.24	Very good
S3	10.92	4.53	18.24	Good
S4	5.99	2.86	29.21	Very good

3.3.2. Antibacterial activity

Antibacterial activity of ZnO nanocomposite treated fabric samples is evaluated in triplicates for each sample through inhibition zone against two different strains of bacteria, Gram-positive (Staphylococcus aureus) and Gram-negative (Escherichia coli). The photographs of these inhibition zones are shown in Figure 6 and their mean diameters are presented in Table 6. Based on the obtained results, it is found that:

(a) All treated samples showed inhibition zones against both types of bacteria.
(b) Against the same bacterium, the inhibition zones of S2 and S4 samples are larger than those of S1 and S3, respectively, this variation is attributed to the variation in the size of the nanocomposites i.e. smaller particles have larger surface area, which provides more contact on bacterial cell membrane, leading to better bactericidal effect [56]. This is in agreement with previously obtained results
(c) The antibacterial activity of the treated samples against S. aureus was higher than against E.coli.

The possible documented mechanism is the electrostatic interaction between the positively charged cationic sites of antibacterial agents (ZnO nanocomposite) with the negatively charged surface membrane of bacteria, causing a change in its permeability and respiration [57]. Also, enabling nanoparticles of smaller size to penetrate the cell membrane and bind with the functional group (–SH) of proteins, causing protein denaturation which inhibits bacterial cell growth and ultimately death. While, nanoparticles of larger size can form a film on the outer membrane surface, obstructing the exchange of nutrients and leading to bacterial cell death [58, 59]. The higher antibacterial activity against Gram +ve (S. aureus) than Gram –ve (E. coli) can be explained according to the differences in cell wall structure between them. The cell wall of Gram-positive bacteria consists of a thick peptidoglycan layer associated with teichoic acids. The teichoic acid backbone is highly charged with the negatively charged phosphate groups, which can establish electrostatic interaction with the positively charged antibacterial agent. While, the cell wall in Gram-negative bacteria consists of a thin layer of peptidoglycan and an additional outer membrane made of lipopolysaccharide. This membrane may be act as an extra barrier against the action of ZnO nanocomposite, making the Gram-negative bacteria less permeable [60-62]. So, ZnO nanocomposites can interact with the cell wall of S. aureus bacteria easier than that of E. coli.

3.3.3. Comfort and mechanical characteristics

Table 7 shows the performance properties of ZnO nanocomposite treated fabric samples like air permeability, water absorbance, antistatic and bursting strength. For each sample, three measurements from different positions are taken and their average is calculated. It is observed that the air permeability of all treated knitted polyester samples was lower than the untreated ones, indicating the deposition of ZnO nanocomposites into the fabric pores through which air could pass. Also, the air permeability of S2 and S4 samples is lower than S1 and S3 due to more ZnO nanocomposites are deposited at pH8. It is seen that depositing ZnO nanocomposites onto the fabric only slightly reduces the air permeability. However, the resultant total air permeability is still within an acceptable range for practical applications [63].

It is clear that there is an improvement in both antistatic and water absorbency properties in all treated samples, this is attributed to the extra hydroxyl and amino groups introduced into samples from either HEMC or CS which increase the fabric's ability to

absorb more water and this is compatible with FTIR results which confirmed that the intensity of O-H band is increased in the samples after treatment. In addition, the effect of ZnO Nps on the fabric roughness i.e. more deposition of ZnO nanocomposites into the fabric samples leads to an increase in its surface roughness and consequently increases the water absorbency [64]. On the other hand, ZnO has the ability to dissipate the accumulated static charge on the fabric because it is an electrically conductive material [65]. While, the bursting strength was slightly decreased (<10%) compared with the untreated fabric.

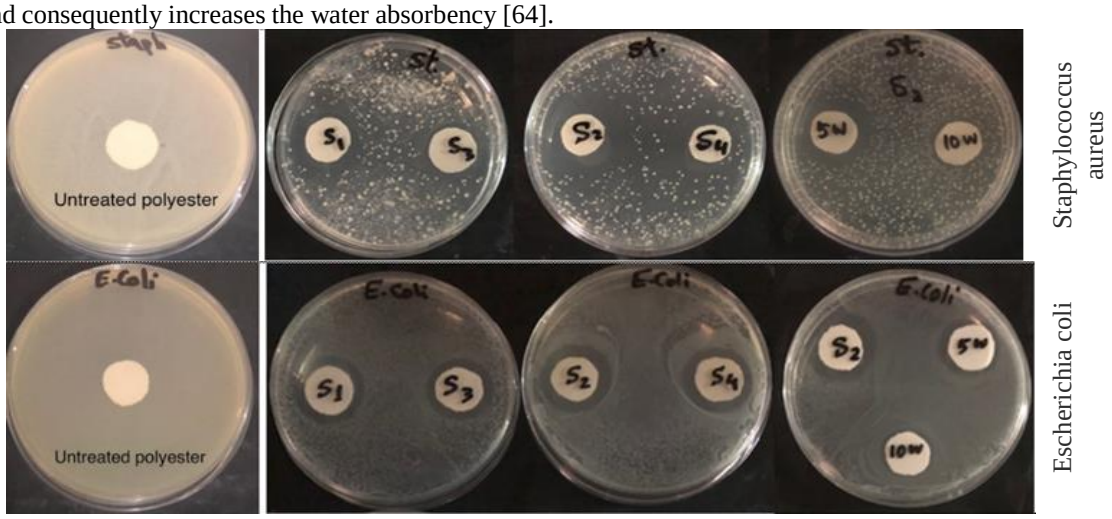

Figure 6. Photographs of the antibacterial activity of untreated and ZnO nanocomposite treated fabric samples (S1, S2, S3 & S4) against two strains of bacteria S. aureus and E. coli

Table 6. The mean diameter of inhibition zone (mm) of the examined samples against S. aureus and E. coli before and after washing.

Sample Code	Mean diameter of inhibition zone (mm)					
	S. Aureus (Gram +ve)			E. Coli (Gram –ve)		
	Before Washing	After Washing		Before Washing	After Washing	
		5 Cycles (5w)	10 Cycles (10w)		5 Cycles (5w)	10 Cycles (10w)
Untreated	0	0	0	0	0	0
S1	25	18.5	15.5	21.5	16	15
S2	36	25	18.1	25	20.5	18
S3	23	17.5	15	20.5	16	15
S4	32	22.5	17.5	24	19	17

Table7. Physicomechanical properties of ZnO nanocomposite treated fabric Samples.

Test	Sample code	Values
Air permeability $Cm^3/Cm^2/S$	Untreated	131
	S1	105
	S2	85.9
	S3	97.6
	S4	78.9
Water absorbency (S)	Untreated	80
	S1	24.6
	S2	6
	S3	54
	S4	47.3
Antistatic property (Kv)	Untreated	0.4
	S1	0.03
	S2	0.005
	S3	0.02
	S4	0.01
Bursting strength (Kgf)	Untreated	89.5
	S1	88.7
	S2	82.4
	S3	86.2
	S4	81.8

4. Conclusion

In this study, we reported an easy, rapid, inexpensive and novel one-pot way for functionalization of knitted polyester fabric with green synthesized ZnO nanocomposites using natural reagents and green physical techniques. Aloe Vera gel extract is used as a reducing agent and two natural biopolymers (HEMC and CS) are used as matrices. The microwave technique was used to assist the formation of nanocomposites, while the ultrasonic technique was used for deposition the synthesized ZnO nanocomposites into polyester fabric. The synthesized ZnO nanocomposites in the reaction mixtures are characterized using UV-Vis spectroscopy and TEM analysis that showed a surface plasmon resonance behaviour and the average size of the synthesized nanoparticles was in the range of 4-54 nm with a spherical shape. While, the functionalized fabric

samples are characterized using SEM, XRD, FTIR and AAS analysis which confirmed the successful deposition of the synthesized ZnO nanocomposites into the fabric samples, resulting in an improvement in its performance properties such as UV blocking, water absorbency and antistatic. In addition, ZnO nanocomposite treated fabric samples showed good antibacterial activity against two strains of bacteria (S. aureus and E. coli). The influence of pH on the synthesized ZnO nanocomposites and the finished fabric samples was evaluated. The above findings prove that the use of microwave and ultrasound are considered a promising alternative techniques for reducing energy, hazardous chemicals and time involved in nanoparticles synthesis and finishing process. Moreover, the obtained functionalized polyester samples can be applied widely in various areas, such as functional clothing, medical and technical textiles.

Conflicts of interest

There are no conflicts to declare.

5. Reference

1. Alharthi M. N., Ismail I., Bellucci S., and Salam M. A. Green synthesis of zinc oxide nanoparticles by Ziziphus jujuba leaves extract: Environmental application, kinetic and thermodynamic studies. *Journal of Physics and Chemistry of Solids*, **158**, 110237 (2021).
2. Gebre S. H. and Sendeku M. G. New frontiers in the biosynthesis of metal oxide nanoparticles and their environmental applications: an overview. *SN Applied Sciences*, **1**(8), 1-28 (2019).
3. Santhoshkumar J., Kumar S. V. and Rajeshkumar S., Synthesis of zinc oxide nanoparticles using plant leaf extract against urinary tract infection pathogen. *Resource-Efficient Technologies*, **3**(4), 459-465 (2017).
4. Parthasarathy G., Saroja M. and Venkatachalam M., Bio-synthesized nano-formulation of zinc oxide-Aloe Vera and to study their characterization and antibacterial activities against multiple pathogens. *International Journal of Pharmaceutical Sciences and Research*, **8**(2), 900 (2017).
5. Naseer M., Aslam U., Khalid B. and Chen B., Green route to synthesize Zinc Oxide Nanoparticles using leaf extracts of Cassia fistula and Melia azadarach and their antibacterial potential. *Scientific Reports*, **10**(1), 1-10 (2020).
6. Shamhari N. M., Wee B. S., Chin S. F. and Kok K. Y., Synthesis and characterization of zinc oxide nanoparticles with small particle size distribution. *Acta Chimica Slovenica*, **65**(3), 578-585 (2018).
7. Chan Y.Y., Pang Y.L., Lim S. and Chong W.C., Facile green synthesis of ZnO nanoparticles using natural-based materials: Properties, mechanism, surface modification and application. *Journal of Environmental Chemical Engineering*, 9(4), 105417 (2021).
8. Abou Elmaaty T., Abdelaziz E., Nasser D., Abdelfattah K., Elkadi S. and El-Nagar K. I., Microwave and Nanotechnology Advanced Solutions to Improve Ecofriendly Cotton's Coloration and Performance Properties. *Egyptian Journal of Chemistry*, **61**(3), 493-502 (2018).
9. Rajendran N. K., George B. P., Houreld N. N. and Abrahamse H., Synthesis of zinc oxide nanoparticles using Rubus fairholmianus root extract and their activity against pathogenic bacteria. *Molecules*, **26**(10), 3029 (2021).
10. Ibrahim N. A., Eid B. M., Abd El-Ghany N. A. and Mabrouk E. M., Polyfunctional cotton cellulose fabric using proper biopolymers and active ingredients. *The Journal of the Textile Institute*, **111**(3), 381-393 (2019).
11. Nobahar A., Carlier J. D., Miguel M. G. and Costa M. C., A review of plant metabolites with metal interaction capacity: a green approach for industrial applications. *BioMetals*, **34**(4), 761-793 (2021).
12. Ovais M., Khalil A. T., Islam N. U., Ahmad I., Ayaz M., Saravanan M. and Mukherjee S., Role of plant phytochemicals and microbial enzymes in the biosynthesis of metallic nanoparticles. *Applied microbiology and biotechnology*, **102**(16), 6799-6814 (2018).
13. Jamkhande P. G., Ghule N. W., Bamer A. H. and Kalaskar M. G., Metal nanoparticles synthesis: An overview on methods of preparation, advantages and disadvantages, and applications. *Journal of drug delivery science and technology*, **53**, 101174 (2019).
14. Alharthi M. N., Ismail I., Bellucci S., and Salam M. A. Green synthesis of zinc oxide nanoparticles by Ziziphus jujuba leaves extract: Environmental application, kinetic and thermodynamic studies. *Journal of Physics and Chemistry of Solids*, **158**, 110237 (2021).
15. Gebre S. H. and Sendeku M. G. New frontiers in the biosynthesis of metal oxide nanoparticles and their environmental applications: an overview. *SN Applied Sciences*, **1**(8), 1-28 (2019).
16. Santhoshkumar J., Kumar S. V. and Rajeshkumar S., Synthesis of zinc oxide nanoparticles using plant leaf extract against urinary tract infection pathogen. *Resource-Efficient Technologies*, **3**(4), 459-465 (2017).
17. Parthasarathy G., Saroja M. and Venkatachalam M., Bio-synthesized nano-formulation of zinc oxide-Aloe Vera and to study their characterization and antibacterial activities against multiple pathogens. *International Journal of Pharmaceutical Sciences and Research*, **8**(2), 900 (2017).
18. Naseer M., Aslam U., Khalid B. and Chen B., Green route to synthesize Zinc Oxide Nanoparticles using leaf extracts of Cassia fistula and Melia azadarach and their antibacterial potential. *Scientific Reports*, **10**(1), 1-10 (2020).
19. Shamhari N. M., Wee B. S., Chin S. F. and Kok K. Y., Synthesis and characterization of zinc oxide nanoparticles with small particle size distribution. *Acta Chimica Slovenica*, **65**(3), 578-585 (2018).
20. Chan Y.Y., Pang Y.L., Lim S. and Chong W.C., Facile green synthesis of ZnO nanoparticles using natural-based materials: Properties, mechanism, surface modification and application. *Journal of*

Environmental Chemical Engineering, 9(4), 105417 (2021).

21. Abou Elmaaty T., Abdelaziz E., Nasser D., Abdelfattah K., Elkadi S. and El-Nagar K. I., Microwave and Nanotechnology Advanced Solutions to Improve Ecofriendly Cotton's Coloration and Performance Properties. *Egyptian Journal of Chemistry*, **61**(3), 493-502 (2018).
22. Rajendran N. K., George B. P., Houreld N. N. and Abrahamse H., Synthesis of zinc oxide nanoparticles using Rubus fairholmianus root extract and their activity against pathogenic bacteria. *Molecules*, **26**(10), 3029 (2021).
23. Ibrahim N. A., Eid B. M., Abd El-Ghany N. A. and Mabrouk E. M., Polyfunctional cotton cellulose fabric using proper biopolymers and active ingredients. *The Journal of the Textile Institute*, **111**(3), 381-393 (2019).
24. Nobahar A., Carlier J. D., Miguel M. G. and Costa M. C., A review of plant metabolites with metal interaction capacity: a green approach for industrial applications. *BioMetals*, **34**(4), 761-793 (2021).
25. Ovais M., Khalil A. T., Islam N. U., Ahmad I., Ayaz M., Saravanan M. and Mukherjee S., Role of plant phytochemicals and microbial enzymes in the biosynthesis of metallic nanoparticles. *Applied microbiology and biotechnology*, **102**(16), 6799-6814 (2018).
26. Jamkhande P. G., Ghule N. W., Bamer A. H. and Kalaskar M. G., Metal nanoparticles synthesis: An overview on methods of preparation, advantages and disadvantages, and applications. *Journal of drug delivery science and technology*, **53**, 101174 (2019).
27. Kwiczak-Yiğitbaşı J., Demir M., Ahan R. E., Canlı S., Şafak Şeker U. O. and Baytekin B., Ultrasonication for environmentally friendly preparation of antimicrobial and catalytically active nanocomposites of cellulosic textiles. *ACS Sustainable Chemistry & Engineering*, **8**(51), 18879-18888 (2020).
28. Abu-Jdayil B., Mourad A. H. I., Hussain A. and Al Abdallah H., Thermal insulation and mechanical characteristics of polyester filled with date seed wastes. *Construction and Building Materials*, **315**, 125805 (2022).
29. Turakhia B., Divakara M. B., Santosh M. S. and Shah S., Green synthesis of copper oxide nanoparticles: a promising approach in the development of antibacterial textiles. *Journal of Coatings Technology and Research*, **17**(2), 531-540 (2020).
30. Raza Z. A. and Anwar F., Impregnation of zinc oxide mediated chitosan nano-composites on polyester fabric for performance characteristics. *Fibers and Polymers*, **17**(9), 1378-1383 (2016).
31. Ramesh M., Anbuvannan M. and Viruthagiri G., Green synthesis of ZnO nanoparticles using Solanum nigrum leaf extract and their antibacterial activity. *Spectrochimica Acta Part A: Molecular and Biomolecular Spectroscopy*, **136**, 864-870 (2015).
32. Yang T., Xiong X., Mishra R., Novák J. and Militký J., Acoustic evaluation of Struto nonwovens and their relationship with thermal properties. *Textile Research Journal*, **88**(4), 426-437 (2018).
33. Bhat G. and Messiry M. E., Effect of microfiber layers on acoustical absorptive properties of nonwoven fabrics. *Journal of Industrial Textiles*, **50**(3), 312-332 (2020).
34. Agarwal R., Jassal M. and Agrawal A. K., Durable functionalization of polyethylene terephthalate fabrics using metal oxides nanoparticles. *Colloids and Surfaces A: Physicochemical and Engineering Aspects*, **615**, 126223 (2021).
35. Chaudhary A., Kumar N., Kumar R. and Salar R. K., Antimicrobial activity of zinc oxide nanoparticles synthesized from Aloe vera peel extract. *SN Applied Sciences*, **1**(1), 1-9 (2019).
36. Senthilkumar N., Nandhakumar E., Priya P., Soni D., Vimalan M. and Potheher I.V., Synthesis of ZnO nanoparticles using leaf extract of Tectona grandis (L.) and their anti-bacterial, anti-arthritic, anti-oxidant and in vitro cytotoxicity activities. *New Journal of Chemistry*, 41(18), 10347-10356 (2017).
37. Kwabena D. E. and Aquisman A. E., Morphology of green synthesized ZnO nanoparticles using low temperature hydrothermal technique from aqueous Carica papaya extract. *Nanoscience and Nanotechnology*, **9**(1), 29-36 (2019).
38. Ajitha B., Reddy Y. A. K. and Reddy P. S., Enhanced antimicrobial activity of silver nanoparticles with controlled particle size by pH variation. *Powder Technology*, **269**, 110-117 (2015).
39. Begum R., Farooqi Z. H., Naseem K., Ali F., Batool M., Xiao J. and Irfan A., Applications of UV/Vis spectroscopy in characterization and catalytic activity of noble metal nanoparticles fabricated in responsive polymer microgels: a review. *Critical reviews in analytical chemistry*, **48**(6), 503-516 (2018).
40. Amirjani A., Koochak N. N. and Haghshenas D. F., Investigating the shape and size-dependent optical properties of silver nanostructures using UV–vis spectroscopy. *Journal of Chemical Education*, **96**(11), 2584-2589 (2019).
41. Türemen M., Demir A. and Gokce Y., The synthesis and application of chitosan coated ZnO nanorods for multifunctional cotton fabrics. *Materials Chemistry and Physics*, **268**, 124736 (2021).
42. Shao D. and Wei Q., Microwave-assisted rapid preparation of nano-ZnO/Ag composite functionalized polyester nonwoven membrane for improving its UV shielding and antibacterial properties. *Materials*, **11**(8), 1412 (2018).
43. Thambidurai S., Gowthaman P., Venkatachalam M. and Suresh S., Natural sunlight assisted photocatalytic degradation of methylene blue by spherical zinc oxide nanoparticles prepared by facile chemical co-precipitation method. *Optik*, **207**, 163865 (2020).
44. Arumugam J., Thambidurai S., Suresh S., Selvapandiyan M., Kandasamy M., Pugazhenthiran N. and Quero F., Green synthesis of zinc oxide nanoparticles using Ficus carica leaf extract and their bactericidal and photocatalytic performance evaluation. *Chemical Physics Letters*, **783**, 139040 (2021).
45. Haque F. Z., Nandanwar R. and Singh P., Evaluating photodegradation properties of anatase and rutile TiO2 nanoparticles for organic compounds. *Optik*, **128**, 191-200 (2017).
46. Duarte L. J. and Bruns R. E., Atomic Polarizations, Not Charges, Determine CH Out-of-Plane Bending Intensities of Benzene Molecules. *The Journal of Physical Chemistry A*, **122**(51), 9833-9841 (2018).

47. Koto N. and Soegijono B., Effect of rice husk ash filler of resistance against of high-speed projectile impact on polyester-fiberglass double panel composites. In *Journal of Physics: Conference Series*, **1191** (1), 012058 (2019).
48. Jain D., Pareek S., Chattopadhyay S. and Behera D., Ni-Doped ZnO-Chitin Composites for Anti-Corrosive Coating on Zn Alloy in Simulated Body Fluid Solution. *Journal of Bio-and Tribo-Corrosion*, **6**(4), 1-13 (2020).
49. Rather L. J., Shabbir M., Li Q. and Mohammad F., Coloration, UV protective, and antioxidant finishing of wool fabric via natural dye extracts: cleaner production of bioactive textiles. *Environmental Progress & Sustainable Energy*, **38**(5), 13187 (2019).
50. Alebeid O. K. and Zhao T., Review on: developing UV protection for cotton fabric. *The Journal of the Textile Institute*, 108(12), 2027-2039 (2017).
51. Ibrahim H.I., Farouk R., El-karadly E.A., Elwahy A.H. and Mousa, A., Synthesis, characterization and application of reactive UV absorbers for enhancing UV protective properties of cotton fabric. *Egyptian Journal of Chemistry*, 63(2), 525-536 (2020).
52. Ramadan M.A., Taha G.M. and EL-Mohr W.Z.E.A., Antimicrobial and UV protection finishing of Polysaccharide-Based Textiles using Biopolymer and AgNPs. *Egyptian Journal of Chemistry*, 63(7), 2707-2716 (2020).
53. Elgory Z.M., Seddik K.M., Yahia M. and El-Gabry L.K., The enhancement of the functional properties of polyester microfiber single jersey using some nano-materials. *Egyptian Journal of Chemistry*, 63(1), 145-154 (2020).
54. Elapasery M., Yassin F.A. and Abdellatif M.E., Nano ZnO Provides Multifunctional on Dyed Polyester Fabrics with Enaminone-Based Disperse Dyes. *Egyptian Journal of Chemistry*, 65(6), 1-2 (2022).
55. Ibrahim N. A., Nada A. A., Eid B. M., Al-Moghazy M., Hassabo A. G. and Abou-Zeid N. Y., Nano-structured metal oxides: synthesis, characterization and application for multifunctional cotton fabric. *Advances in Natural Sciences: Nanoscience and Nanotechnology*, **9**(3), 035014 (2018).
56. Dong Y., Zhu H., Shen Y., Zhang W. and Zhang, L., Antibacterial activity of silver nanoparticles of different particle size against Vibrio Natriegens. *Plos One*, **14**(9), 0222322 (2019).
57. El-Shafei A., Shaaraw S., Motawe F.H. and Refaei R., Herbal extract as an ecofriendly antibacterial finishing of cotton fabric. *Egyptian Journal of Chemistry*, 61(2), 317-327 (2018).
58. Yan D., Li Y., Liu Y., Li N., Zhang X. and Yan C., Antimicrobial Properties of Chitosan and Chitosan Derivatives in the Treatment of Enteric Infections. *Molecules*, **26**(23), 7136 (2021).
59. Nisar P., Ali N., Rahman L., Ali M. and Shinwari Z. K., Antimicrobial activities of biologically synthesized metal nanoparticles: an insight into the mechanism of action. *JBIC Journal of Biological Inorganic Chemistry*, **24**(7), 929-941(2019).
60. Román L. E., Gomez E. D., Solís J. L. and Gómez M. M., Antibacterial cotton fabric functionalized with copper oxide nanoparticles. *Molecules*, **25**(24), 5802 (2020).
61. Yusof N. A. , Zain N. M. and Pauzi N., Synthesis of ZnO nanoparticles with chitosan as stabilizing agent and their antibacterial properties against Gram-positive and Gram-negative bacteria. *International journal of biological macromolecules*, **124**, 1132-1136 (2019).
62. Piva D. H., Piva R. H., Rocha M. C., Dias J. A., Montedo O. R. K., Malavazi I. and Morelli M. R. Antibacterial and photocatalytic activity of ZnO nanoparticles from Zn (OH) 2 dehydrated by azeotropic distillation, freeze drying, and ethanol washing. *Advanced Powder Technology*, **28**(2), 463-472 (2017).
63. 63Abd Alhalim, S., Mabrouk, M., Kanawy Ibrahim, S., H Hamdy, N. and Ramadan, A., Synthesis and Physicomechanical Studies of Nano ZnO Coated Textile fabrics. *Egyptian Journal of Chemistry*, 63(2), 625-631(2020).
64. Nourbakhsh S., Montazer M. and Khandaghabadi Z., Zinc oxide nanoparticles coating on polyester fabric functionalized through alkali treatment. *Journal of Industrial Textiles*, **47**(6), 1006-1023 (2018).
65. Temesgen A. G., Turşucular Ö. F., Eren R. and Ulcay Y., Novel applications of nanotechnology in modification of textile fabrics properties and apparel. *International Journal of Advanced Multidisciplinary Research*, **5**(12), 49-58 (2018).